

Cite this: DOI: 00.0000/xxxxxxxxxx

Detection of sub-degree fluctuations of the local cell membrane slope using optical tweezers

Rahul Vaippully,^a Vaibavi Ramanujan,^b Manoj Gopalakrishnan,^a Saumendra Bajpai,^b and Basudev Roy^a

Received Date

Accepted Date

DOI: 00.0000/xxxxxxxxxx

Normal thermal fluctuations of the cell membrane have been studied extensively using high resolution microscopy and focused light, particularly at the peripheral regions of a cell. We use a single probe particle attached non-specifically to the cell-membrane to determine that the power spectral density is proportional to (frequency)^{-5/3} in the range of 5 Hz to 1 kHz. We also use a new technique to simultaneously ascertain the slope fluctuations of the membrane by relying upon the determination of pitch motion of the birefringent probe particle trapped in linearly polarized optical tweezers. In the process, we also develop the technique to identify pitch rotation to a high resolution using optical tweezers. We find that the power spectrum of slope fluctuations is proportional to (frequency)⁻¹, which we also explain theoretically. We find that we can extract parameters like bending rigidity directly from the coefficient of the power spectrum particularly at high frequencies, instead of being convoluted with other parameters, thereby improving the accuracy of estimation. We anticipate this technique for determination of the pitch angle in spherical particles to high resolution as a starting point for many interesting studies using the optical tweezers.

Rheology of the cell membrane assumes significance in cell migration, adhesion, differentiation and development¹⁻⁴, not to mention, also in probing the health of the cell. It is directly influenced in diseases like malaria⁵ and sickle cell anaemia⁶. Further, the cancer cells are softer and more elastic compared to healthy ones to help in intravasation⁷, when trying to get into the blood vessels and spread through the body, where the exact mechanism by which it changes the elasticity is not known⁸. In view of all these facets, study of membrane stiffness and the subsequent response to external perturbations assume enormous importance.

Membrane fluctuations are inherent to many membrane processes, like ion-pump functioning, vesicle budding and trafficking⁹⁻¹¹ in living cells. Our knowledge of the mechanisms of the membrane processes shall be significantly improved while learning about the nature of active fluctuations^{12,13} in membranes.

Typically, the normal membrane fluctuations have been studied to ascertain the rheological parameters of the living cells¹³. These fluctuations are powered by thermal energy as well as ATP dependent processes. The temporal range of such fluctuations is quite broad, starting from slow (10 sec) actin waves to drive large wavelength fluctuations (100 nm to 10 μm) at cell edges and basal membrane¹⁴⁻¹⁶, to relatively smaller amplitude ones

(5 to 50 nm) which appear at the basal membrane^{17,18} and are mainly thermal in nature. Fluctuations of the basal membrane, as opposed to the cell edges have not been explored much due to requirements of high resolution. We use a new technique where we place a particle on top of a cell membrane at locations away from the cell edges to find the normal fluctuations after ensuring non-specific binding. This does not require proximity to a second surface as the interference is between the unscattered light in photonic force microscopy with that of the scattered light from the particle¹⁹⁻²¹, and thus the unconfined free surface of the cell can also be probed.

Here we introduce a hitherto new concept, that of membrane local slope fluctuations, to study the parameters. To perform such a measurement, we show how the pitch-rotation angle²² of a spherical particle attached to the membrane can be ascertained at high resolution in optical tweezers to add additional parameters that can greatly improve the accuracy. We show that such measurement provides information of the parameters like bending rigidity directly instead of being ascertained in a convoluted form with other parameters. In the process, we show for the first time, a method to determine the pitch rotation angle to a high resolution using optical tweezers.

1 Theory

The pitch signal is given as the difference-in-halves signal of the light scattered by the birefringent particle placed inside crossed

^a Department of Physics, Indian Institute of Technology Madras, Chennai, India, 600036 E-mail: basudev@iitm.ac.in

^b Department of Applied Mechanics, Indian Institute of Technology Madras, Chennai, India, 600036

polarizers²², and can also extend to particles trapped in optical tweezers. The pitch signal is linearly proportional to the difference-in-halves signal. The power spectrum due to pitch Brownian motion is given as follows, in consistency with the conventional power spectra in optical tweezers²³.

$$PSD = \frac{A}{\omega^2 + B} \quad (1)$$

Further, following the Wiener-Khinchin theorem, the power spectral density (PSD) of membrane height fluctuations is given by

$$PSD_z = \int dt e^{i\omega t} \int \frac{d^2 \mathbf{q} d^2 \mathbf{q}'}{(2\pi)^4} \langle h_{\mathbf{q}}(0) h_{\mathbf{q}'}(t) \rangle \quad (2)$$

where $h_{\mathbf{q}}(t) = \int d^2 \mathbf{r} e^{i\mathbf{q} \cdot \mathbf{r}} h(\mathbf{r}, t)$ is the Fourier transform of the height fluctuation, whose auto-correlation is

$$\langle h_{\mathbf{q}}(0) h_{\mathbf{q}'}(t) \rangle = 4\pi^2 F(q) \delta(\mathbf{q} + \mathbf{q}') e^{-\omega_q t} \quad (3)$$

where

$$F(q) = \frac{k_B T}{\kappa q^4 + \sigma q^2} \quad (4)$$

from equipartition theorem, where κ is the bending modulus and σ is the surface tension of the membrane. Assuming an impermeable, flat cell membrane which separates two fluids of mean viscosity η , the wavelength relaxation rate ω_q is given by²⁴⁻²⁶

$$\omega_q = \frac{\kappa q^4 + \sigma q^2}{4\eta q} \quad (5)$$

After using (3) in (2), and switching to plane polar coordinates, it follows that

$$PSD_z = \frac{1}{\pi} \int_{q_{\min}}^{q_{\max}} dq q F(q) \frac{\omega_q}{\omega_q^2 + \omega^2} \quad (6)$$

If we consider the cell has an infinite membrane with a point like detection area, $q_{\min} = 0$ and $q_{\max} = \infty$ in (3). Next, after using (4) and (5) in (3), it follows that the Z-power spectral density of a particle stuck on the membrane is

$$PSD_z = \frac{4\eta k_B T}{\pi} \int_0^\infty \frac{dq}{(\kappa q^3 + \sigma q)^2 + (4\eta \omega)^2} \quad (7)$$

In the low frequency limit, ie., when $\omega \rightarrow 0$, it can be shown that

$$PSD_z \sim \frac{k_B T}{2\sigma \omega} \quad (\omega \rightarrow 0), \quad (8)$$

whereas in the large ω limit, we find

$$PSD_z \sim \frac{k_B T}{3(4\eta^2 \kappa)^{1/3} \omega^{5/3}} \quad (\omega \rightarrow \infty). \quad (9)$$

The expression in (9) suggests that the Z-power spectrum obeys a power-law decay at large frequencies ω , with an exponent $-5/3$

Consider a birefringent particle stuck on the cell membrane, which is characterised by height fluctuations $h(\mathbf{r}, t)$, where $\mathbf{r} =$

(x, y) are points on the plane of projection, which we define as the $x - y$ plane.

The slope of the optic axis at a particular instant in the h-r plane is given by,

$$\tan(\theta) = \frac{h_2 - h_1}{r_2 - r_1} \quad (10)$$

where the particle touches the cell membrane between r_1 and r_2 , such that $r_2 - r_1$ is the length of the contact for the particle. This is of the order of 100 nm for a 1 μm diameter particle and is assumed to remain constant during rotational motion.

For small angles θ , we may approximate $\tan \theta \approx \theta$. Within this approximation, the appropriate generalisation of (10) for the two-dimensional membrane surface is

$$\theta(\mathbf{r}, t) = \partial_r h(\mathbf{r}, t), \quad (11)$$

where \mathbf{r} is the location of the centre of the particle in the $x - y$ plane. In terms of the Fourier transform $h_{\mathbf{q}}(t)$, the angle θ becomes

$$\theta(\mathbf{r}, t) = -\frac{i}{(2\pi)^2} \int d^2 \mathbf{q} h_{\mathbf{q}}(t) q \cos \phi e^{-i\mathbf{q} \cdot \mathbf{r}}, \quad (12)$$

where ϕ is the angle between the (fixed) vector \mathbf{r} and \mathbf{q} . After using the auto-correlation for the height field given in (3) and carrying out the angular integration, the auto-correlation of the angle becomes

$$\langle \theta(\mathbf{r}, 0) \theta(\mathbf{r}, t) \rangle = \frac{1}{4\pi} \int dq q^3 F(q) e^{-\omega_q t} \quad (13)$$

where the function $F(q)$ has been given in (4). Upon substituting the latter in (13), and using the Wiener-Khinchin theorem, the PSD for the angle/slope fluctuations is found have the general form

$$PSD_\theta = \frac{2\eta k_B T}{\pi} \int dq \frac{q^2}{(\kappa q^3 + \sigma q)^2 + (4\eta \omega)^2} \quad (14)$$

After a careful analysis of the integral, we find that the low frequency and high frequency behaviours of (14) are given by

$$PSD_\theta = \frac{8k_B T \eta}{3\pi \sqrt{\sigma^3 \kappa}} - \frac{4k_B T \eta^2}{\sigma^3} \omega \quad (\omega \rightarrow 0) \quad (15)$$

$$PSD_\theta = \frac{k_B T}{12\kappa \omega} \quad (\omega \rightarrow \infty) \quad (16)$$

Thus, we find the functional relationships for the PSD for pitch motion at low and high frequencies.

2 Experimental details

The experiment was performed using an optical tweezers kit OTKB/M (Thorlabs, USA) in an inverted configuration, where a linearly polarized 1.7 W, 1064 nm wavelength diode laser (Laserer, China) was used to form the optical tweezers. The objective was an Olympus 100X, 1.3 NA oil immersion one with the illumination aperture being overfilled and the condenser being a 10x, 0.25 NA Nikon air-immersion one. The power of laser light at the sample plane was set to be about 100 mW. The schematic diagram has been shown in Fig. 1. An LED lamp illuminates

the sample from the top using a dichroic mirror, while another dichroic collects the visible light to be placed in a CMOS camera (Thorlabs). The forward scattered light emerges through the top dichroic and is sent into a polarizing beam splitter, where most of the light through one of the ports and sent into a Quadrant Photodiode (QPD). The other arm experiences a minimum in scattered intensity and experiences a complete dark when there are no particles in the trapping region.

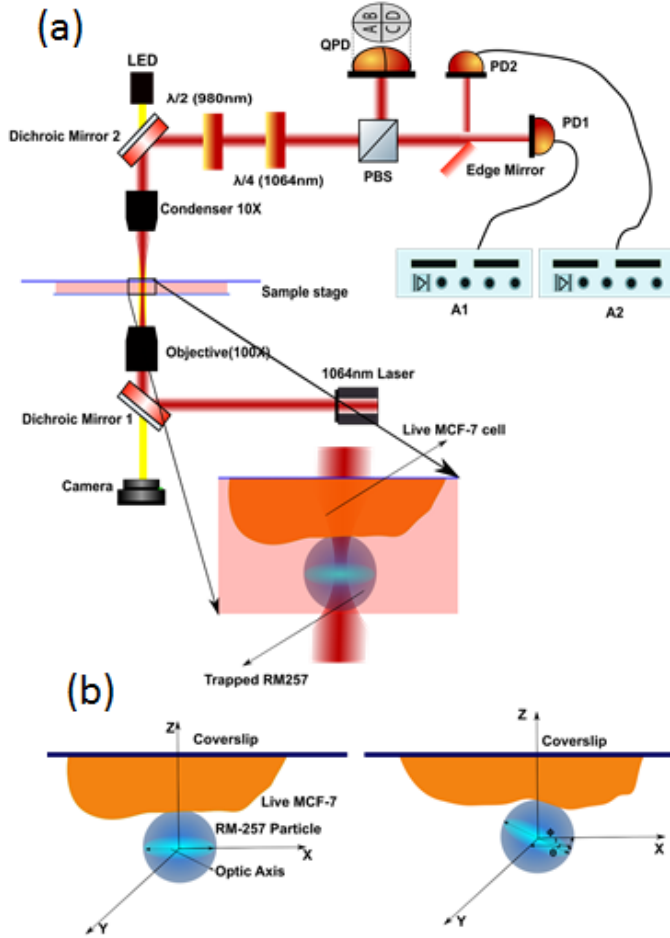


Fig. 1 (a) Schematic diagram of the set-up used to detect pitch rotation. A very well polarized 1064 nm laser beam is used to trap the particle, which then passes through into the forward scatter direction. The component of the forward scattered light orthogonal to the input polarization is sent into an edge mirror to ascertain the asymmetry in the scatter pattern. (b) The pitch rotation detection technique is used to find the local slope fluctuations of the cell membrane as shown in this cartoon.

The tracer particles that we used are birefringent liquid crystalline RM257 (Merck) particles made using standard techniques^{27,28} and of typical diameter $1 \pm 0.1 \mu\text{m}$. When these particles are trapped in optical tweezers, the birefringence axis aligns with that of the polarization of light, both in the conventional yaw and the pitch sense. When a well-linearly polarized light is used to trap a birefringent particle, some amount of light also emerges from the dark port of the polarizing beam splitter placed in the forward direction, due to the internal structure of the directors of the particle resulting in a four-lobe scatter inten-

sity pattern. It has been shown in²² that the distribution of light in between these halves becomes anisotropic when the particle turns in the pitch sense. We exploit this very facet to ascertain the pitch motion.

We place an edge mirror in the path of the dark port of the polarizing beam splitter (PBS) in the forward direction and send one half of the scattered light into one photodiode (PD1), while sending the other half to a different photodiode (PD2). These photodiode signals are amplified with current amplifiers and then sent into the Data Acquisition System (DAQ card, National Instruments). These time series signals from PD1 and PD2 are then subtracted to gain the pitch signal. The advantage of using this configuration, as opposed to another QPD, is that larger gains can be obtained here.

Typical X, Z and pitch power spectra for a birefringent particle trapped in water are shown in Fig. 2.

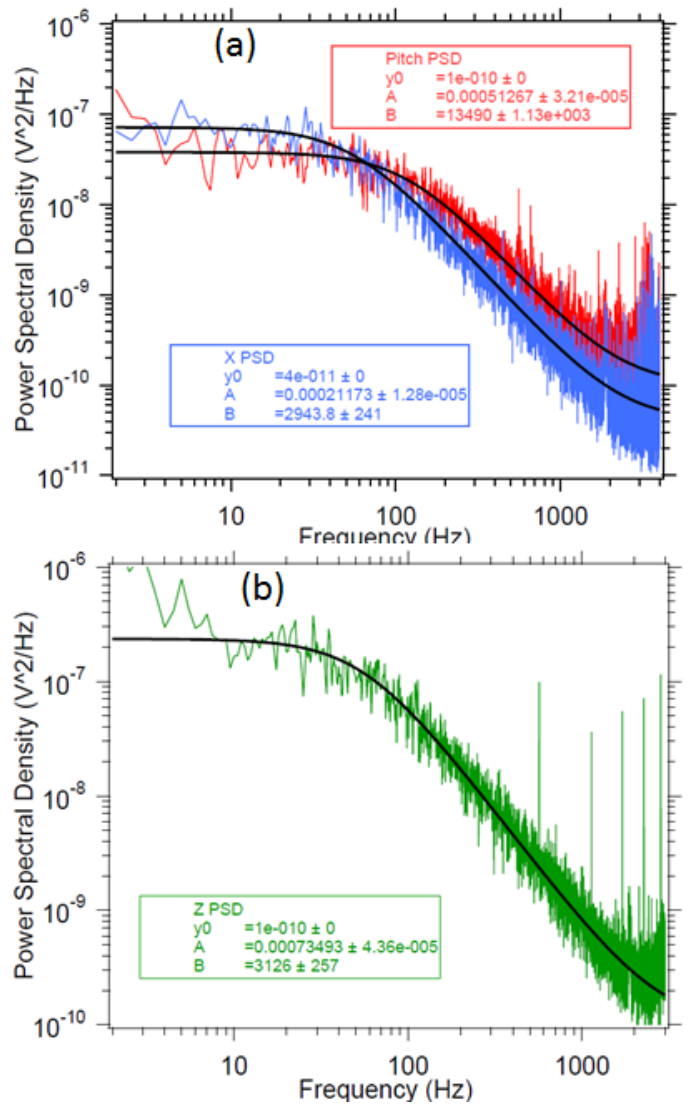


Fig. 2 The power spectra for (a) the pitch motion and the transverse x motion (b) for the axial Z motion, fitted to lorentzians (eq. (1)) for calibration purposes.

The X and Z PSD are the usual lorentzian in nature, the pitch

spectra is also found to be a good Lorentzian. This can be used for calibrating the pitch motion using eq. (1)²³.

Michigan Cancer Foundation-7 (MCF-7) cells were grown on glass slides coated with gelatin. These slides were initially treated with the piranha solution and sterilized with a UV (265nm) lamp for 20 minutes and thereafter coated with 0.5% gelatin solution. MCF7 cells were added towards the center of the coverslip and the Dulbecco's Modified Eagle Medium (DMEM) supplemented with 10% fetal bovine serum and 1% glutamine-penicillin-streptomycin was added on top of the coverslip. 10 μ L of birefringent sample with particles suspended in water was added to the cells. Cells were incubated at 5% carbondioxide and 37 C.

One such birefringent particle was trapped and gradually brought in contact with the cell surface and held for about 10 seconds. It is observed that the particle attaches to the cell by forming non-specific binding to present us with an excellent opportunity to probe the fluctuations of the cell membrane²⁹. We simultaneously probe the slope fluctuations of the membrane from the light scattered by the birefringent particle while in contact with the membrane, as explained in eq. (15).

3 Results and discussions

The power spectral density of the motion of the particle normal to the membrane and the slope fluctuations are reported in Fig. 3.

The Fig. 3(a) indicates the PSD for the normal motion of the cell membrane. We find this to fit well to a power law with exponent $-\frac{5}{3}^{12}$, particularly at high frequencies between 10 Hz and 1 KHz. This is consistent with the theory presented in eq. (9) for normal fluctuations, thereby indicating that the particle is indeed attached to the cell membrane and probing the normal fluctuations. We simultaneously ascertain the slope fluctuation PSD and show in Fig. 3(b). This PSD fits well to a power law and shows an exponent of 1.25 ± 0.16 , which we call the pitch PSD. Calibrating the pitch motion amplitude with factors from Fig. 2, we find ourselves capable of resolving 100 mdeg at 40 Hz. We also show the noise floor in Fig. 3(b) (green curve). The amplitude of the power law is $1 \pm 0.3 \text{ deg}^2$.

In order to ascertain the accuracy of the power law when fitted to the pitch PSD, we block average³⁰ the PSD data in exponents of 2 (namely 1,2,4,8 and so on). This block averaged PSD also fits well to the power law, within 5% error, till about 5 Hz but starts deviating upon using lower frequencies, with the exponent being 1.22 ± 0.15 , as shown in Fig. 4.

We also show the statistics of pitch exponents observed in our experiments in Fig. 5.

The average value of the pitch exponent is obtained to be -1.15 ± 0.12 . This exponent is comparable with the expected pitch exponent of -1, as indicated in eq. (15), and consistent to a p-value of 0.0001.

We also show, in Fig. 6, that the value of the bending rigidity estimated from the measurement of the slope is coming to be $1.88 \pm 0.42 \times 10^{-19}$ J, which is consistent with literature values¹³. The curves for the normal and slope fluctuations can be simultaneously used to ascertain the bending rigidity, the cytoplasmic

viscosity and the surface tension at high accuracy.

4 Conclusions

Thus to conclude, we have developed a new technique to ascertain the pitch rotational motion to a high sensitivity using optical tweezers. The pitch power spectrum for a birefringent particle trapped in water fits well to a Lorentzian. This particle can be attached non-specifically to a cell membrane by holding it against the membrane for 10 seconds. As soon as the particle attaches to the membrane, the vertical fluctuations of the particle can be used to find the membrane fluctuations. The PSD of the vertical fluctuations shows a power law exponent of $-\frac{5}{3}$, confirming that the particle is indeed recording the normal membrane fluctuations. We simultaneously ascertain the slope fluctuations of the membrane and find that the PSD fits well to a power law with the exponent consistent to -1 within 2 standard deviations.

Acknowledgements

We thank the Indian Institute of Technology Madras for their seed and initiation grants.

Notes and references

- 1 J. T. Parsons, A. R. Horwitz and M. A. Schwartz, *Nat. Rev. Mol. Cell Biol.*, 2010, **11**, 633–643.
- 2 T. Lecuit and P. F. Lenne, *Nat. Rev. Mol. Cell Biol.*, 2007, **8**, 633–644.
- 3 H. T. McMahon and J. T. Gallop, *Nature*, 2005, **438**, 590–596.
- 4 J. Kim, H. Jo, H. Hong, M. H. Kim, J. K. Lee, W. D. Heo and J. Kim, *Nat. Comm.*, 2015, **6**, 6781.
- 5 Y. Park, M. Diez-Silva, G. Popescu, G. Lykotrafitis, W. Choi, M. S. Feld and S. Suresh, *Proc. Nat. Acad. Sci. (USA)*, 2008, **105**, 13730–13735.
- 6 P. Connes, T. Alexy, J. Detterich, M. Romana, M.-D. Hardy-Dessources and S. K. Ballas, *Blood Rev.*, 2016, **30**, 111–118.
- 7 D. Wirtz, K. Konstantopoulos and P. C. Searson, *Nat. Rev. Cancer*, 2011, **11**, 512–522.
- 8 S. E. Winograd-Katz, R. Fassler, B. Geiger and K. R. Legate, *Nat. Rev. Mol. Cell Biol.*, 2014, **15**, 273–288.
- 9 N. Gov, A. G. Zilman and S. Safran, *Phys. Rev. Lett.*, 2003, **90**, 228101.
- 10 N. S. Gov and S. A. Safran, *Biophys. J.*, 2005, **88**, 1859–1874.
- 11 Y. Park, C. A. Best, K. Badizadegan, R. R. Dasari, M. S. Feld, T. Kuriabova, M. L. Henle, A. J. Levine and G. Popescu, *Proc. Nat. Acad. Sci. (USA)*, 2010, **107**, 6731–6736.
- 12 H. Yu, Y. Yang, Y. Yang, F. Zhang, S. Wang and N. Tao, *Nanoscale*, 2018, **10**, 5133–5139.
- 13 A. Biswas, A. Alex and B. Sinha, *Biophys. J.*, 2017, **113**, 1768–1781.
- 14 G. Giannone, B. J. Dubin-Thaler, H.-G. Dobereiner, N. Kieffer, A. R. Bresnick and M. P. Sheetz, *Cell*, 2004, **116**, 441–443.
- 15 H.-G. Dobereiner, B. J. Dubin-Thaler, J. M. Hofman, H. S. Xenias, T. N. Sims, G. Giannone, M. L. Dustin, C. H. Wiggins and M. P. Sheetz, *Phys. Rev. Lett.*, 2006, **97**, 038102.
- 16 C.-H. Chen, F.-C. Tsai, C.-C. Wang and C.-H. Lee, *Phys. Rev. Lett.*, 2009, **103**, 238101.

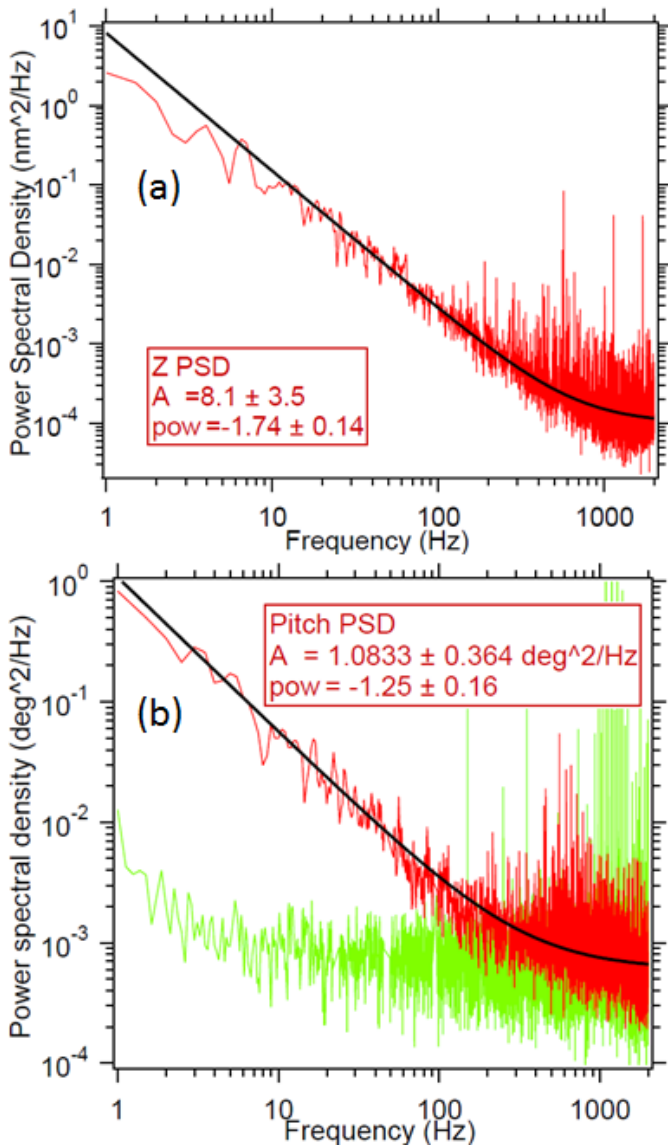


Fig. 3 The calibrated Power Spectral Densities (PSD) for (a) the normal fluctuations of the membrane (b) the local slope fluctuations of the membrane indicated by the Pitch angle. In (b), the background PSD with the particle placed on a solid glass surface (without membrane fluctuations) is shown in green.

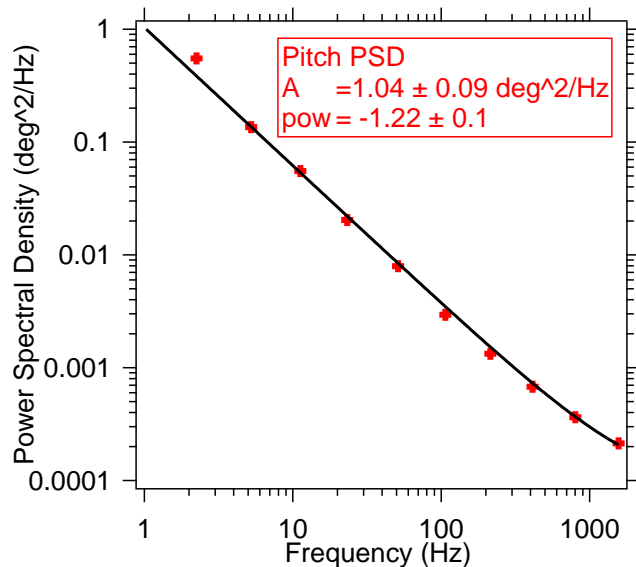


Fig. 4 A pitch PSD data for a particle placed on the cell membrane is shown here. The data has been averaged in logarithmic blocks and then

- 17 C. Monzel, D. Schmidt, C. Kleusch, D. Kirchenbuchler, U. Seifert, A.-S. Smith, K. Sengupta and R. Merkel, *Nat. Commun.*, 2015, **6**, 8162.
- 18 M. C. D. Santos, R. Deturche, C. Vezy and R. Jaffiol, *Biophys. J.*, 2016, **111**, 1316–1327.
- 19 E.-L. Florin, A. Pralle, J. K. H. Horber and E. H. K. Stelzer, *J. Struct. Biol.*, 1997, **119**, 202–211.
- 20 L. Friedrich and A. Rohrbach, *Nat. Nano.*, 2015, **10**, 1064–1069.
- 21 F. Junger, F. Kohler, A. Meinel, T. Meyer, R. Nitschke, B. Erhard and A. Rohrbach, *Biophys. J.*, 2015, **109**, 869–882.
- 22 B. Roy, A. Ramaiya and E. Schaffer, *J. Opt.*, 2018, **20**, 035603.
- 23 E. Schaffer, S. F. Norrelykke and J. Howard, *Langmuir*, 2007, **23**, 3654–3665.
- 24 S. Ramaswamy, J. Toner and J. Prost, *Pramana*, 1999, **53**, 237–242.
- 25 J. Prost, J.-B. Manneville and R. Bruinsma, *Eur. Phys. J. B*, 1998, **1**, 465–480.
- 26 U. Siefert, *Phys. Rev. E*, 1994, **49**, 3124–3127.
- 27 A. Ramaiya, B. Roy, M. Bugiel and E. Schaffer, *Proc. Nat. Acad. Sci. (USA)*, 2017, **114**, 10894–10899.
- 28 R. Vaippully, D. Bhatt, A. D. Ranjan and B. Roy, *Phys. Scr.*, 2019, **94**, 105008.
- 29 R. Vaippully, V. Ramanujan, S. Bajpai and B. Roy, *J. Phys. Cond. Mat.*, 2020, **32**, 235101.

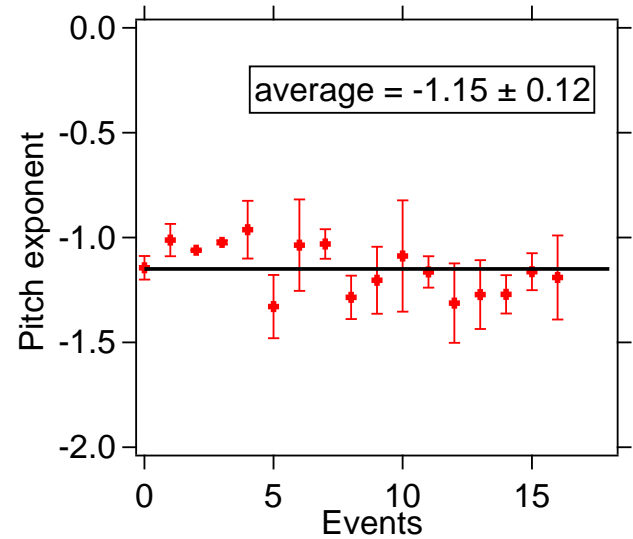
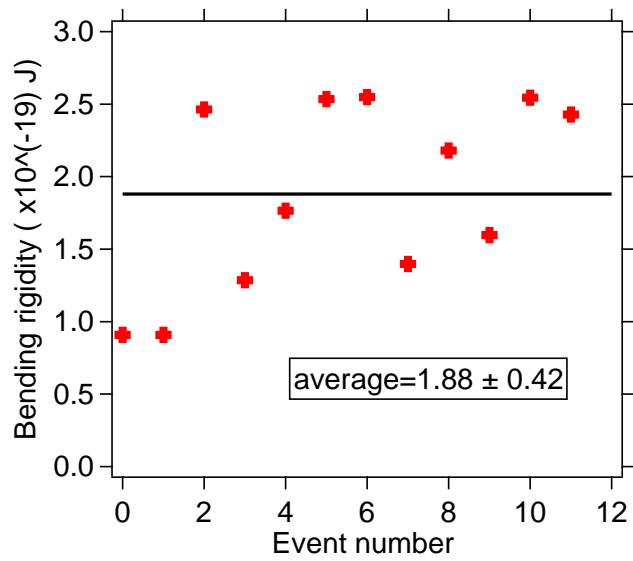


Fig. 5 The variation of pitch exponents for different measurement events. The average value of the exponent to the power law fit is -1.15 ± 0.12 , consistent to -1 with a p-value of 0.0001.



30 K. Berg-Sorensen and H. Flyvberg, *Rev. Sci. Instrum.*, 2004, 75, 594–612.

Fig. 6 This figure shows the variation of the calculated bending rigidity from the amplitudes of the power laws fitted to the high frequency region of the pitch PSD. The values are consistent with the values previously mentioned in the literature.